Synthesis and Redox Studies on Ruthenium and Osmium Complexes with Primary and Secondary Phosphines. Single-crystal Structures of *trans*-[RuCl₂(PPhH₂)₄] and *trans*-[OsCl₂(PPh₂H)₄]·CH₂Cl₂†

Alexander J. Blake,[a] Neil R. Champness,[b] Robin J. Forder,[b] Christopher S. Frampton,[c] Carole A. Frost,[b] Gillian Reid[*,b] and Rachel H. Simpson[b]

[a] *Department of Chemistry, The University of Edinburgh, West Mains Road, Edinburgh EH9 3JJ, UK*

[b] *Department of Chemistry, The University of Southampton, Highfield, Southampton SO9 5NH, UK*

[c] *Roche Research Centre, Welwyn Garden City AL7 3AY, UK*

Reaction of $RuCl_3 \cdot 3H_2O$ or $[NH_4]_2[OsCl_6]$ with 5–7 molar equivalents of PR_2H (R = Ph or C_6H_{11}) or $PPhH_2$ in degassed refluxing EtOH solution (or EtOH–water for Os) gave $[MCl_2(PR_2H)_4]$ and $[MCl_2(PPhH_2)_4]$ in high yield as yellow solids. Ultraviolet–visible and ^{31}P NMR spectroscopic studies confirm that these species exist as *trans* isomers in solution and the integrity of the PH functions. Prolonged standing of *trans*-$[RuCl_2(PPh_2H)_4]$ in CH_2Cl_2 solution led to partial isomerisation to the *cis* isomer as confirmed by ^{31}P NMR spectroscopy. The crystal structure of *trans*-$[RuCl_2(PPhH_2)_4]$ has been determined. It confirms a *trans* arrangement of the Cl^- ligands with the Ru^{II} occupying a crystallographic inversion centre with four precisely coplanar equatorial $PPhH_2$ ligands, Ru–Cl 2.422(3), Ru–P(1) 2.319(3) and Ru–P(2) 2.318(3) Å. The lower steric demands of the $PPhH_2$ ligands compared to PPh_2H are reflected in the more regular octahedral arrangement seen in *trans*-$[RuCl_2(PPhH_2)_4]$ compared to *trans*-$[RuCl_2(PPh_2H)_4] \cdot 0.5CHCl_3$. The crystal-structure determination of *trans*-$[OsCl_2(PPh_2H)_4] \cdot CH_2Cl_2$ showed two independent half molecules in the asymmetric unit with each Os^{II} occupying an inversion centre and co-ordinated to a *trans* arrangement of two Cl^- and four PPh_2H ligands, Os(1)–Cl 2.448(2), Os(2)–Cl 2.443(2), Os(1)–P 2.357(2), 2.349(2), Os(2)–P 2.355(2), 2.333(2) Å. With the exception of $[RuCl_2(PPhH_2)_4]$ (irreversible), cyclic voltammetric studies on the complexes *trans*-$[MCl_2(PR_2H)_4]$ and *trans*-$[MCl_2(PPhH_2)_4]$ show a reversible oxidation in each case, which is assigned to a M^{II}–M^{III} redox couple.

We have been investigating the co-ordination chemistry of primary and secondary phosphines (PRH_2 and PR_2H) with transition-metal ions. Our interest arises from the fact that they offer the possibility of further functionalisation following co-ordination, as shown for example by Stelzer and co-workers[1] in their template syntheses of tetraphosphine macrocycles. In order for these primary and secondary phosphine complexes to be useful for further functionalisation, such as alkylation, at the PH groups, it is essential that they can be synthesised in good yields initially with the PH groups intact, thereby allowing controlled deprotonation and further reaction. Despite the vast literature describing tertiary phosphine (PR_3) co-ordination, PRH_2 and PR_2H ligation have been relatively poorly studied,[2-8] and early studies indicated that upon co-ordination the P–H bonds become unstable to deprotonation yielding phosphido-species.[3] Pregosin and co-workers[4] have recently reported the first example of an agostic Pd · · · H–P interaction in the complex cation $[Pd_2(\mu\text{-}PBu^t_2)(\mu\text{-}PBu^t_2H)(PBu^t_2H)_2]^+$.

We have recently reported the complex cations $[MCl\{P(C_6H_{11})_2H\}_3]^+$ (M = Pd or Pt) which were shown by multinuclear NMR spectroscopy to be stable with respect to deprotonation in solution over very long periods.[5] In contrast, PPh_2H complexes of Pd^{II} and Pt^{II} undergo spontaneous deprotonation to give the phosphido dimers $[M_2Cl_2(\mu\text{-}PPh_2)_2(PPh_2H)_2]$.[3] As part of our studies were intended to establish the susceptibility of PR_2H and PRH_2 complexes to spontaneous deprotonation we have extended this work to ruthenium and osmium complexes. We

now report the synthesis and redox studies of $[MCl_2(PR_2H)_4]$ and $[MCl_2(PPhH_2)_4]$, (M = Ru or Os, R = Ph or C_6H_{11}). Single-crystal structure determinations on *trans*-$[RuCl_2(PPhH_2)_4]$ and *trans*-$[OsCl_2(PPh_2H)_4] \cdot CH_2Cl_2$ are also described. The syntheses of *trans*-$[MCl_2(PPh_2H)_4]$ and related complexes have been reported previously by Sanders,[6] and the crystal structure of *trans*-$[RuCl_2(PPh_2H)_4] \cdot 0.5CHCl_3$ by Stephenson and co-workers.[7]

Results and Discussion

Reaction of $RuCl_3 \cdot 3H_2O$ with an excess (5–7 molar equivalents) of PPh_2H or $PPhH_2$ in degassed, refluxing EtOH under N_2 for *ca.* 2 h yielded the tetrakis(phosphine) complex $[RuCl_2(PPh_2H)_4]$ or $[RuCl_2(PPhH_2)_4]$ in high yield. Similarly, reaction of $[NH_4]_2[OsCl_6]$ with 5–7 molar equivalents of primary or secondary phosphine in refluxing aqueous EtOH solution under N_2 afforded $[OsCl_2(PR_2H)_4]$ (R = Ph or C_6H_{11}) and $[OsCl_2(PPhH_2)_4]$. Following recrystallisation from CH_2Cl_2–Et_2O these complexes were characterised by IR, UV/VIS, ^1H and ^{31}P NMR spectroscopies, FAB mass spectrometry and microanalyses. In each case the IR spectrum shows, in addition to peaks due to phenyl or cyclohexyl groups as appropriate, a weak feature at *ca.* 2340 cm^{-1} assigned to a co-ordinated PH function.
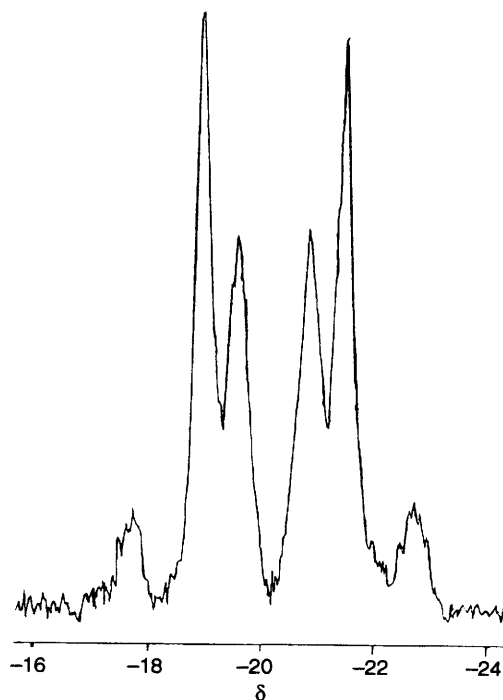
The FAB mass spectra of the products show peaks with the correct isotopic pattern for $[RuCl_2(PPh_2H)_4 - H]^+$ (*m/z* 915), $[RuCl_2(PPhH_2)_4 - H]^+$ (611), $[OsCl_2(PPh_2H)_4 + 2H]^+$ (1008), $[OsCl_2\{P(C_6H_{11})_2H\}_4 + H]^+$ (1055) and $[OsCl_2(PPhH_2)_4]^+$ (702). In each case a very distinctive fragmentation pattern involving successive loss of chloride and phosphine ligands is also apparent, with no evidence for higher-molecular-

---

† *Supplementary data available:* see Instructions for Authors, *J. Chem. Soc., Dalton Trans.*, 1994, Issue 1, pp. xxiii–xxviii.

Table 1 Selected spectroscopic and electrochemical data

Complex	$\delta(^{31}P)^a$	$\nu_{max}\ (\varepsilon_{mol})^b$	$E_{\frac{1}{2}}(M^{II}-M^{III})^c$
trans-[RuCl$_2$(PPh$_2$H)$_4$]	18.0	32 900 (3430), 28 250(sh) (1 100), 22 300 (310)	+0.30
cis-[RuCl$_2$(PPh$_2$H)$_4$]	26.6^d	—	—
	36.7^d		
trans-[RuCl$_2$(PPhH$_2$)$_4$]	−25.0	30 300(sh) (1 140), 23 300 (190)	+0.55^e
trans-[OsCl$_2$(PPh$_2$H)$_4$]	−17.7	26 180(sh) (580), 22 320 (120)	+0.03
trans-[OsCl$_2$\{P(C$_6$H$_{11}$)$_2$H\}$_4$]	−31.0	31 300 (975), 23 900(sh) (350), 18 200 (195)	−0.37
trans-[OsCl$_2$(PPhH$_2$)$_4$]	−61.4	33 900(sh) (720), 30 670 (610)	+0.07

^{a} In ppm relative to 85% H$_3$PO$_4$, measured in CH$_2$Cl$_2$-CDCl$_3$ at 300 K. ^{b} In cm^{-1} (ε_{mol} in dm^3 mol^{-1} cm^{-1}), measured as fresh solutions in CH$_2$Cl$_2$; sh = shoulder. ^{c} In Volts vs. ferrocene–ferrocenium (0 V), measured at 200 mV s^{-1} in CH$_2$Cl$_2$. ^{d} Triplet, $^3J_{PP}$ 30 Hz. ^{e} Irreversible, E_{pa} quoted.

Fig. 1 The ^{31}P NMR spectrum of *trans*-[OsCl$_2$(PPh$_2$H)$_4$] (145.8 MHz, CH$_2$Cl$_2$-CDCl$_3$, 300 K)

Table 2 Selected bond lengths (Å) and angles (°) for *trans*-[RuCl$_2$(PPhH$_2$)$_4$]

Ru–Cl	2.422(3)	P(1)–C(1P)	1.823(5)
Ru–P(1)	2.319(3)	P(2)–C(7P)	1.811(7)
Ru–P(2)	2.318(3)		
P(1)–Ru–P(2)	89.99(10)	Ru–P(1)–C(1P)	121.5(3)
Cl–Ru–P(2)	89.12(10)	Ru–P(2)–C(7P)	120.1(2)
Cl–Ru–P(1)	91.83(9)		
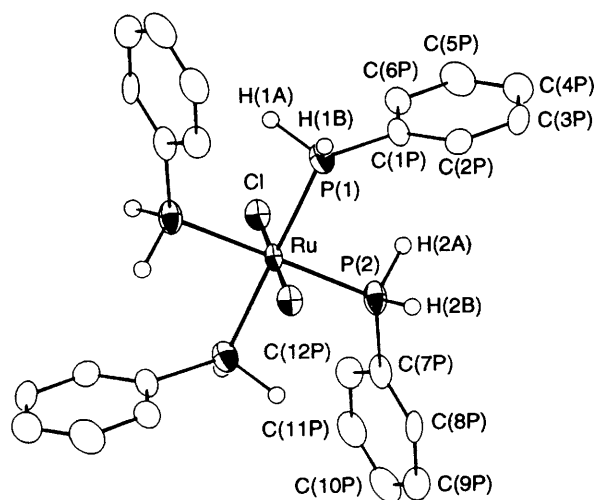
Fig. 2 View of the structure of *trans*-[RuCl$_2$(PPhH$_2$)$_4$] with the numbering scheme adopted; H atoms are omitted for clarity

weight species such as dimers. Previous work on tertiary phosphine complexes of ruthenium and osmium has indicated a strong tendency for formation of dimeric halide-bridged species.[9] This does not appear to be the case for the primary and secondary phosphine complexes in this study, except for the reaction between RuCl$_3$·3H$_2$O with P(C$_6$H$_{11}$)$_2$H (see below). We have also seen some evidence from FAB mass spectrometry for the formation of the pentakis complex [OsCl(PPhH$_2$)$_5$]$^+$ (*m/z* 777). This species may be formed in the 3-nitrobenzyl alcohol matrix \{it is not seen in the ^{31}P NMR spectrum of [OsCl$_2$(PPhH$_2$)$_4$]\}, but work is underway to investigate these higher P : M ratio species.

The ^{31}P-\{^{1}H\} NMR spectroscopic studies (Table 1) confirm that the complexes exist as *trans* isomers in the fresh samples studied, each of which exhibits a singlet shifted significantly downfield relative to the free primary or secondary phosphine. The proton-coupled ^{31}P NMR spectra each reveal second-order patterns (Fig. 1) arising from a large one-bond P–H coupling together with *cis* and *trans* three-bond P–H couplings and coupling to the phenyl or cyclohexyl protons. These data also confirm retention of the PH functions in all of the PR$_2$H and PRH$_2$ complexes. Upon standing in CH$_2$Cl$_2$ solution for several days some *trans* to *cis* isomerisation occurs for [RuCl$_2$-(PPh$_2$H)$_4$], with the appearance of two triplets in the ^{31}P-\{^{1}H\} NMR spectrum, at δ 26.6 (P *trans* P) and 36.7 (P *trans* Cl), with $^2J_{PP}$ 30 Hz.

In view of the lack of characterised examples of metal complexes incorporating primary and secondary phosphines, and to establish the bond-length and -angle distributions, single-crystal structure analyses on *trans*-[RuCl$_2$(PPhH$_2$)$_4$] and *trans*-[OsCl$_2$(PPhH$_2$)$_4$]·CH$_2$Cl$_2$ were undertaken. Suitable crystals of [RuCl$_2$(PPhH$_2$)$_4$] were obtained by slow diffusion of diethyl ether into a cooled solution of the complex in CH$_2$Cl$_2$. The structure of [RuCl$_2$(PPhH$_2$)$_4$] (Fig. 2) is centrosymmetric with the ruthenium(II) ion on a crystallographic inversion centre with *trans*-dichloride and four equatorial PPhH$_2$ ligands, Ru–Cl 2.422(3), Ru–P(1) 2.319(3) and Ru–P(2) 2.318(3) Å (Table 2). The phenyl groups adopt a propeller-like arrangement, with the four PPhH$_2$ ligands lying in a precisely planar arrangement around the Ru^{II} with no significant distortions of the Cl–Ru–P or P–Ru–P angles from 90°. The structure of *trans*-[RuCl$_2$-(PPh$_2$H)$_4$]·0.5CHCl$_3$ shows Ru–Cl 2.4317(8), Ru–P 2.3505(8), 2.3665(8) Å.[7] The steric requirements in *trans*-[RuCl$_2$-(PPhH$_2$)$_4$] are considerably less than for [RuCl$_2$(PPh$_2$H)$_4$] [the Tolman cone angle θ(PPh$_2$H) = 128, θ(PPhH$_2$) = 110°], and this is seen in the bond-angle distributions around the Ru^{II}. The complex [RuCl$_2$(PPh$_2$H)$_4$] shows rather distorted Cl–Ru–P angles of 87.13(3) and 82.00(3)° and a *cis*-P–Ru–P angle of 90.34(3)°. Thus, the chloride ligands are tilted away from the

apical site, probably due to the presence of two Ph groups on each P atom in this complex.[7] To our knowledge, trans-[RuCl$_2$(PPhH$_2$)$_4$] is the first structurally characterised example of a tetrakis(primary phosphine) complex. Cotton et al.[8] reported the structure of the secondary phosphine complex [RuCl$_2$(PMe$_2$H)$_4$], which also exhibits a trans-dichloro arrangement, with Ru–Cl 2.440(1), Ru–P 2.323(1), 2.331(1) Å.

Comparison of the related ruthenium(II) species [RuCl$_2$-(PPhH$_2$)$_4$], [RuCl$_2$(PPh$_2$H)$_4$] and the five-co-ordinate complex [RuCl$_2$(PPh$_3$)$_3$] [Ru–P trans to P 2.374(6), 2.412(6) Å],[10] shows that the metal–phosphorus bond lengths increase by approximately 0.03 Å upon replacement of the P-bound H atoms by phenyl groups in the series PPhH$_2$, PPh$_2$H, PPh$_3$.

Small single crystals of trans-[OsCl$_2$(PPh$_2$H)$_4$]·CH$_2$Cl$_2$ were obtained by slow evaporation from a solution of the complex in CH$_2$Cl$_2$. The single-crystal structure shows two independent half molecules of [OsCl$_2$(PPh$_2$H)$_4$] and a CH$_2$Cl$_2$ solvent molecule in the asymmetric unit, with each Os^{II} occupying a crystallographic inversion centre. The stereochemistry at Os^{II} (Fig. 3) is distorted octahedral with trans-dichoro ligands, Os(1)–Cl(1) 2.448(2), Os(1)–P(1) 2.357(2), Os(1)–P(2) 2.349(2),

Table 3 Selected bond lengths (Å) and angles (°) for trans-[OsCl$_2$(PPh$_2$H)$_4$]

Os(1)–Cl(1)	2.448(2)	Os(2)–Cl(2)	2.443(2)
Os(1)–P(1)	2.357(2)	Os(2)–P(3)	2.355(2)
Os(1)–P(2)	2.349(2)	Os(2)–P(4)	2.333(2)
P(1)–C(6)	1.822(9)	P(1)–C(12)	1.838(9)
P(2)–C(18)	1.825(9)	P(2)–C(24)	1.835(8)
P(3)–C(30)	1.844(8)	P(3)–C(36)	1.814(8)
P(4)–C(42)	1.827(8)	P(4)–C(48)	1.824(8)
P(1)–H(1)	1.28	P(2)–H(2)	1.28
P(3)–H(23)	1.42	P(4)–H(24)	1.38
Cl(1)–Os(1)–P(1)	82.86(8)	Cl(2)–Os(2)–P(3)	99.00(7)
Cl(1)–Os(1)–P(2)	88.58(8)	Cl(2)–Os(2)–P(4)	87.25(8)
P(1)–Os(1)–P(2)	90.37(8)	P(3)–Os(2)–P(4)	90.78(8)
Os(1)–P(1)–C(6)	123.4(3)	Os(1)–P(1)–C(12)	121.7(3)
C(6)–P(1)–C(12)	102.0(4)	Os(1)–P(2)–C(18)	121.5(3)
Os(1)–P(2)–C(24)	121.3(3)	C(18)–P(2)–C(24)	99.3(4)
Os(2)–P(3)–C(30)	120.1(3)	Os(2)–P(3)–C(36)	125.4(3)
C(30)–P(3)–C(36)	100.9(4)	Os(2)–P(4)–C(42)	119.2(3)
Os(2)–P(4)–C(48)	122.9(3)	C(42)–P(4)–C(48)	101.5(4)

Os(2)–Cl(2) 2.443(2), Os(2)–P(3) 2.355(2) and Os(2)–P(4) 2.333(2) Å (Table 3). These bond lengths are slightly shorter than in the corresponding trans-[RuCl$_2$(PPh$_2$H)$_4$]·0.5CHCl$_3$,[7] in keeping with the smaller ionic radius of Os^{II}.

Electronic spectroscopic studies were also performed on the complexes trans-[MCl$_2$(PR$_2$H)$_4$] (M = Ru, R = Ph; M = Os, R = Ph or C$_6$H$_{11}$) and [MCl$_2$(PPhH$_2$)$_4$] (M = Ru or Os). These species all exhibit approximate D_{4h} symmetry at M^{II}, and therefore should show two d–d transitions corresponding to $^1A_{1g} \longrightarrow {}^1E_g$ at low frequency and $^1A_{1g} \longrightarrow {}^1A_{2g}$ at higher frequency. All spectra were recorded in freshly prepared CH$_2$Cl$_2$ solutions and the results are given in Table 1.

The redox responses of the complexes of Ru^{II} and Os^{II} measured by cyclic voltammetry in CH$_2$Cl$_2$ solution (0.1 mol dm^{-3} NBu$^n_4$BF$_4$ supporting electrolyte) are presented in Table 1. With the exception of trans-[RuCl$_2$(PPhH$_2$)$_4$] which shows an irreversible oxidation ($E_{pa} = +0.55$ V vs. ferrocene–ferrocenium), a reversible oxidation assigned to a M^{II}–M^{III} couple is observed for each complex, indicating that the metal(III) complexes are also stable with respect to decomposition and deprotonation on the cyclic voltammetry time-scale. We might expect that deprotonation of one or more of the PH functions would occur more readily for the metal(III) complexes since the higher oxidation state would favour phosphide co-ordination. This is consistent with the irreversibility of the Ru^{II}–Ru^{III} couple observed for [RuCl$_2$(PPhH$_2$)$_4$]. As expected, the oxidation potentials for the osmium(II) complexes are significantly less anodic than those of their ruthenium(II) analogues. The ease of oxidation of the former is consistent with the observation that exposure of solutions of these to air leads to the appearance of a red colouration due to the corresponding osmium(III) complexes. Comparison of the oxidation potentials for trans-[MCl$_2$(PPhH$_2$)$_4$] and trans-[MCl$_2$(PPh$_2$H)$_4$] shows that replacing a proton on each phosphine ligand with a phenyl group has a rather small effect, with the M^{II}–M^{III} couple shifting to a slightly more cathodic potential. This contrasts with the anodic shift usually observed upon replacement of a P-bound alkyl substituent with a phenyl group. Thus, for example, the Os^{II}–Os^{III} couple for trans-[OsCl$_2$(dmpe)$_2$] (dmpe = Me$_2$PCH$_2$CH$_2$PMe$_2$) occurs at $E_\frac{1}{2} = +0.04$ V, while for trans-[OsCl$_2$(dppe)$_2$] (dppe = Ph$_2$PCH$_2$CH$_2$PPh$_2$) $E_\frac{1}{2} = +0.28$ V vs. ferrocene–ferrocenium.[11]

We also attempted the synthesis of [RuCl$_2${P(C$_6$H$_{11}$)$_2$H}$_4$] by reaction of RuCl$_3$·3H$_2$O with 5 molar equivalents of P(C$_6$H$_{11}$)$_2$H in degassed EtOH solution. This afforded a yellow solid initially which turned green during the reaction. The IR spectrum of this insoluble product showed the presence of cyclohexyl groups (ν_{CH} 2920, 2850, δ_{CH} 1450 cm^{-1}), P–H functions (ν_{PH} 2300 cm^{-1}) and possibly a Ru–Cl stretch at 320 cm^{-1}. The FAB mass spectrum showed no peak for [RuCl$_2$-{P(C$_6$H$_{11}$)$_2$H}$_4$] (m/z 964) and no fragmentation pattern similar to those seen for the other complexes described. It did however show several low-intensity peaks consistent with dinuclear ruthenium dicyclohexylphosphine species, e.g. m/z 1334 (calc. for [^{102}Ru$_2$^{35}Cl$_4${P(C$_6$H$_{11}$)$_2$H}$_5$]$^+$ 1334). The poor solubility of the product hampered our attempts to record ^{1}H and ^{31}P NMR spectra.
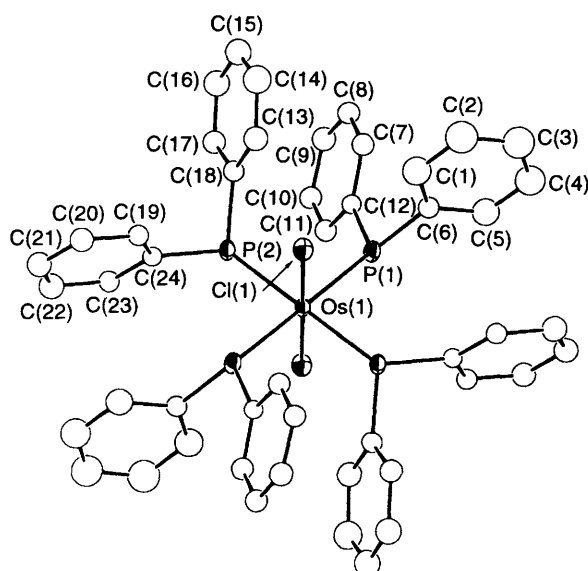

Fig. 3 View of the structure of one of the molecules of trans-[OsCl$_2$(PPh$_2$H)$_4$] in the asymmetric unit with the numbering scheme adopted (the other molecule is essentially indistinguishable); H atoms are omitted for clarity

Experimental

Infrared spectra were measured as KBr or CsI discs using a Perkin-Elmer 983 spectrometer over the range 200–4000 cm^{-1}, mass spectra by electron impact or fast-atom bombardment (FAB) using 3-nitrobenzyl alcohol as matrix on a VG Analytical 70–250 SE spectrometer, solution electronic spectra in quartz cells (path length 1 cm) using a Perkin-Elmer UV/VIS/NIR Lambda 19 spectrometer, ^{1}H NMR spectra using a JEOL FX90 or Bruker AM360 spectrometer operating at 90 or 360 MHz respectively and ^{31}P NMR spectra using a Bruker AM360 spectrometer operating at 145.8 MHz using 10 mm tubes with either a 5 mm D$_2$O insert or the addition of 10–15%

deuteriated solvent as a lock and referenced to 85% H_3PO_4 (δ 0). Microanalyses were performed by the Imperial College microanalytical service. The compound $P(C_6H_{11})_2H$ was obtained from Strem; $PPhH_2$[12] and PPh_2H[13] were prepared as described in the literature.

Cyclic voltammetry experiments were performed using a Model 362 EG & G Princeton Applied Research scanning potentiostat, using a glassy carbon working electrode and platinum wire as auxiliary electrode, with a standard calomel reference electrode and 0.1 mol dm^{-3} tetrabutylammonium tetrafluoroborate in CH_2Cl_2 solution as supporting electrolyte. All potentials are quoted *versus* ferrocene–ferrocenium.

(*a*) *Synthesis of* $[RuCl_2(PPh_2H)_4]$.[6]—This complex was prepared according to the literature method, using $RuCl_3\cdot3H_2O$ (40 mg, 0.153 mmol) and PPh_2H (0.2 cm^3, 1.075 mmol) in EtOH (10 cm^3), yield 75%. (Found: C, 62.2; H, 5.02%. Calc. for $C_{48}H_{44}Cl_2P_4Ru$: C, 62.9; H, 4.85%). FAB mass spectrum: m/z 915, 881, 730, 695, 657, 579, 544, 505, 469, 394, 317 and 285; calc. for $[^{102}Ru^{35}Cl_2(PPh_2H)_4]^+$ 916; the other peaks correspond to fragments formed by loss of PPh_2H ligands and Cl atoms. ^1H NMR (360 MHz, $CDCl_3$, 298 K): δ 7.5–7.0 (m, Ph, 40 H) and 6.26 (m, PH, 4 H). IR (CsI disc): 3030m, 2360w, 1590w, 1580w, 1490m, 1440m, 1190w, 1090m, 1065w, 1020w, 910w, 880m, 850w, 735s, 690s, 610w, 510s, 480m, 450w, 410m and 310w cm^{-1}.

(*b*) *Synthesis of* $[RuCl_2(PPhH_2)_4]$.—Method as for (*a*) using $RuCl_3\cdot3H_2O$ (70 mg, 0.267 mmol) and $PPhH_2$ (0.2 cm^3, 1.818 mmol) in EtOH (20 cm^3), yield 64%. (Found: C, 46.1; H, 4.35%. Calc. for $C_{24}H_{28}Cl_2P_4Ru$: C, 47.1; H, 4.60%). FAB mass spectrum: m/z 611, 576, 501, 467, 427, 392, 357, 318 and 240; calc. for $[^{102}Ru^{35}Cl_2(PPhH_2)_4]^+$ 612; fragmentation by loss of $PPhH_2$ and Cl accounts for all other peaks at lower m/z. ^1H NMR (360 MHz, $CDCl_3$, 298 K): δ 7.6–7.1 (m, Ph, 20 H) and 5.31 (m, PH, 8 H). IR (CsI disc): 3060w, 2340w, 1500w, 1440m, 1100w, 1060w, 930w, 880m, 750m, 700m, 480w, 420m and 320w cm^{-1}.

(*c*) *Single-crystal Structure Determination of trans*-[Ru-$Cl_2(PPhH_2)_4$].—*Crystal data.* $C_{24}H_{28}Cl_2P_4Ru$, $M = 612.34$, monoclinic, space group $C2/c$, $a = 18.642(4)$, $b = 9.892(2)$, $c = 16.177(3)$ Å, β = 117.03(3)°, $U = 2657$ Å^3 [from 2θ values of 27 reflections measured at ±ω (2θ = 24–28°, λ = 0.710 73 Å)], $Z = 4$, $D_c = 1.531$ g cm^{-3}, $T = 150$ K, pale yellow cube, $0.27 \times 0.23 \times 0.21$ mm, μ = 10.30 cm^{-1}, $F(000) = 1240$.

Data collection and processing. Stoë Stadi-4 four-circle diffractometer equipped with Oxford Cryostreams low-temperature device,[14] graphite-monochromated Mo-Kα X-radiation, $T = 150$ K, ω–2θ scans using the learnt-profile method,[15] 1926 data collected (2θ$_{max}$ 45°, h − 20 to 15, k 0–10, l 0–19), semiempirical absorption correction applied (minimum and maximum transmission factors 0.890, 1.000 respectively), 1640 unique (R_{int} 0.066), giving 1407 reflections with $F \geq 6\sigma(F)$ for use in all calculations. No significant crystal decay or movement was observed.

Structure solution and refinement. The positions of all non-H atoms in one half of the $[RuCl_2(PPhH_2)_4]$ molecule were located by direct methods, with the Ru occupying a crystallographic inversion centre at (0,0,0).[16] These non-H atoms were then refined (by least squares on F)[17] with anisotropic thermal parameters, the phenyl groups being refined as rigid groups. Phenyl H atoms were included in fixed, calculated positions, while the P-bound H atoms were located in the difference map and subsequently constrained to have a P–H bond length of 1.40 Å. At final convergence R, $R' = 0.0721$, 0.1046 respectively, $S = 1.179$ for 130 refined parameters and the final ΔF synthesis showed no Δρ above + 1.59 or below − 2.43 e Å^{-3}. Close inspection of the full electron-density map showed that the peak and trough were both within 1 Å of the Ru atom, and there was no substantial residual electron density elsewhere. The weighting scheme $w^{-1} = \sigma^2(F) + 0.002\ 284\ F^2$

Table 4 Fractional atomic coordinates ($\times 10^4$) for *trans*-[RuCl$_2$-(PPhH$_2$)$_4$] with estimated standard deviations (e.s.d.s) in parentheses

Atom	X/a	Y/b	Z/c
Ru	0(0)	0(0)	0(0)
Cl	−386(1)	1864(3)	684(2)
P(1)	−640(1)	964(3)	−1464(2)
C(1P)	−1514(3)	172(7)	−2401(4)
C(2P)	−2291(3)	600(7)	−2608(4)
C(3P)	−2955(3)	13(7)	−3344(4)
C(4P)	−2842(3)	−1000(7)	−3873(4)
C(5P)	−2065(3)	−1427(7)	−3666(4)
C(6P)	−1401(3)	−841(7)	−2930(4)
P(2)	1172(1)	1152(3)	282(2)
C(7P)	1142(4)	2546(5)	−459(4)
C(8P)	651(4)	3653(5)	−539(4)
C(9P)	605(4)	4732(5)	−1116(4)
C(10P)	1049(4)	4703(5)	−1615(4)
C(11P)	1540(4)	3596(5)	−1535(4)
C(12P)	1586(4)	2517(5)	−958(4)

gave satisfactory agreement analyses and in the final cycle (Δ/σ)$_{max}$ was 0.03.

Fractional atomic coordinates are presented in Table 4. Atomic scattering factors were inlaid,[17] or taken from ref. 18. Molecular geometry calculations utilised PARST[19] and Fig. 2 and 3 were produced by ORTEP II.[20]

(*d*) *Synthesis of* $[OsCl_2(PPh_2H)_4]$.—Method as for (*a*) above, using $[NH_4]_2[OsCl_6]$ (95 mg, 0.215 mmol) and PPh_2H (0.2 cm^3, 1.075 mmol) in water–EtOH (1 : 3 v/v, 20 cm^3). (Found: C, 52.4; H, 4.10%. Calc. for $C_{48}H_{44}Cl_2OsP_4\cdot CHCl_3$: C, 52.3; H, 4.05%). FAB mass spectrum: m/z 1008, 971, 820, 785, 634, 596, 519, 483, 442, 406 and 365; calc. for $[^{192}Os^{35}Cl_2(PPh_2H)_4]^+$ 1006; loss of PPh_2H and Cl ligands account for all other peaks. ^1H NMR (360 MHz, $CDCl_3$, 298 K): δ 7.0–7.5 (m, Ph, 40 H) and 5.64 (m, PH, 4 H). IR (CsI disc): 3060w, 2320w, 1490w, 1440m, 1100m, 740m, 700m, 520m, 490w, 460w and 420w cm^{-1}.

(*e*) *Single-crystal Structure Determination of trans*-[OsCl$_2$-(PPh$_2$H)$_4$]·CH$_2$Cl$_2$.—*Crystal data.* $C_{48}H_{44}Cl_2OsP_4\cdot CH_2Cl_2$, $M = 1090.81$, monoclinic, space group $C2/c$, $a = 38.426(3)$, $b = 11.427(4)$, $c = 23.375(3)$ Å, β = 116.247(6)°, $U = 9205$ Å^3 [from 2θ values of 20 reflections measured at ±ω (2θ = 14–21°, λ = 0.710 73 Å)], $Z = 8$, $D_c = 1.574$ g cm^{-3}, $T = 123$ K, orange plate, $0.20 \times 0.09 \times 0.04$ mm, μ = 31.77 cm^{-1}, $F(000) = 4352$.

Data collection and processing. Rigaku AFC7R four-circle diffractometer, graphite-monochromated Mo-Kα X-radiation, $T = 123$ K, ω–2θ scans with ω scan width = (0.79 + 0.35 tan θ)°, 6502 data collected (2θ$_{max}$ 45°, h 0–41, k 0–12, l −25 to 25). Since there were no identifiable faces an empirical absorption correction was applied (ψ scans) (minimum and maximum transmission factors 0.8721, 0.9973 respectively), 6386 unique reflections (R_{int} 0.052), giving 4222 with $F \geq 4\sigma(F)$ for use in all calculations. No significant crystal decay or movement was observed.

Structure solution and refinement. The positions of all non-H atoms in the two half molecules of $[OsCl_2(PPh_2H)_4]$ were located by direct methods, with each Os atom occupying a crystallographic inversion centre.[21] One CH_2Cl_2 solvent molecule was also identified during refinement. The Os, Cl and P atoms were then refined (by least squares on F) with anisotropic thermal parameters, with phenyl H atoms included in fixed, calculated positions; the P-bound H atoms were located in the difference map and their coordinates fixed. At final convergence $R,R' = 0.039$, 0.038 respectively, $S = 1.32$ for 281 refined parameters and the final ΔF synthesis showed no Δρ above + 0.86 or below − 0.80 e Å^{-3}. The weighting scheme

Table 5 Atomic coordinates for trans-$[OsCl_2(PPh_2H)_4] \cdot CH_2Cl_2$ with e.s.d.s. in parentheses

Atom	x	y	z	Atom	x	y	z
Os(1)	0	0	0	C(21)	0.082 6(3)	0.093 7(9)	−0.169 0(4)
Os(2)	0.25	0.25	0.5	C(22)	0.104 1(3)	0.019 8(9)	−0.119 4(4)
Cl(1)	−0.038 56(6)	0.164 7(2)	−0.063 5(1)	C(23)	0.096 8(2)	0.017 2(8)	−0.065 4(4)
Cl(2)	0.182 64(6)	0.206 3(2)	0.426 48(10)	C(24)	0.067 5(2)	0.086 5(8)	−0.063 9(4)
Cl(3)	0.391 2(1)	0.126 7(3)	0.235 4(2)	C(25)	0.217 8(2)	0.540 4(7)	0.605 0(4)
Cl(4)	0.472 7(1)	0.062 8(3)	0.302 5(2)	C(26)	0.224 5(2)	0.657 5(8)	0.624 0(4)
P(1)	0.013 42(7)	0.077 5(2)	0.101 1(1)	C(27)	0.261 8(3)	0.703 0(8)	0.649 9(4)
P(2)	0.057 37(7)	0.083 2(2)	0.005 8(1)	C(28)	0.292 3(2)	0.632 3(8)	0.656 6(4)
P(3)	0.240 78(7)	0.314 4(2)	0.588 0(1)	C(29)	0.285 6(2)	0.514 3(8)	0.637 5(4)
P(4)	0.255 16(7)	0.056 6(2)	0.534 8(1)	C(30)	0.248 3(2)	0.469 7(7)	0.611 9(4)
C(1)	−0.031 3(3)	0.281 0(9)	0.077 4(5)	C(31)	0.163 0(2)	0.254 6(8)	0.554 3(4)
C(2)	−0.054 1(3)	0362(1)	0.090 8(6)	C(32)	0.132 1(2)	0.231 2(8)	0.569 2(4)
C(3)	−0.063 6(3)	0.341(1)	0.141 1(5)	C(33)	0.137 7(2)	0.233 3(8)	0.632 0(4)
C(4)	−0.050 1(3)	0.241(1)	0.177 1(5)	C(34)	0.173 7(2)	0.259 1(8)	0.679 7(4)
C(5)	−0.027 2(3)	0.163 5(9)	0.164 7(5)	C(35)	0.204 8(2)	0.280 0(7)	0.666 5(4)
C(6)	−0.017 7(3)	0.183 6(8)	0.114 3(4)	C(36)	0.199 4(2)	0.279 4(7)	0.602 7(4)
C(7)	0.069 4(2)	0.244 2(9)	0.179 6(4)	C(37)	0.213 3(2)	−0.004 4(9)	0.601 5(4)
C(8)	0.106 5(3)	0.275 8(8)	0.223 3(4)	C(38)	0.207 4(3)	−0.021 6(8)	0.656 4(4)
C(9)	0.135 6(3)	0.196 2(9)	0.242 8(4)	C(39)	0.238 2(3)	−0.004 9(9)	0.715 0(4)
C(10)	0.129 7(3)	0.083 0(8)	0.219 2(4)	C(40)	0.274 1(3)	0.024 1(8)	0.721 7(4)
C(11)	0.092 6(3)	0.049 5(8)	0.176 9(4)	C(41)	0.280 3(2)	0.039 7(7)	0.666 3(4)
C(12)	0.062 1(2)	0.129 2(8)	0.156 1(4)	C(42)	0.249 2(2)	0.023 8(7)	0.606 4(4)
C(13)	0.045 1(3)	0.323 5(9)	0.016 2(4)	C(43)	0.291 3(3)	−0.159 6(8)	0.546 0(4)
C(14)	0.057 0(3)	0.437 7(10)	0.036 1(5)	C(44)	0.320 5(3)	−0.233 9(8)	0.550 8(4)
C(15)	0.095 6(3)	0.459 7(9)	0.076 6(5)	C(45)	0.354 4(3)	−0.190 9(8)	0.552 1(4)
C(16)	0.121 9(3)	0.371 0(9)	0.095 8(5)	C(46)	0.359 9(3)	−0.069 9(9)	0.553 3(4)
C(17)	0.110 8(3)	0.257 1(9)	0.075 6(4)	C(47)	0.330 9(2)	0.004 9(8)	0.549 9(4)
C(18)	0.071 8(3)	0.232 3(8)	0.034 7(4)	C(48)	0.296 0(2)	−0.037 5(7)	0.545 8(4)
C(19)	0.045 8(3)	0.160 3(8)	−0.115 9(4)	C(49)	0.432 9(4)	0.119(1)	0.308 7(6)
C(20)	0.053 8(3)	0.162 1(9)	−0.168 0(4)				

$w^{-1} = \sigma^2(F)$ gave satisfactory agreement analyses and in the final cycle $(\Delta/\sigma)_{max}$ was 0.00.

Fractional atomic coordinates are presented in Table 5.

Additional material available for both structures from the Cambridge Crystallographic Data Centre comprises H-atom coordinates, thermal parameters and remaining bond lengths and angles.

(*f*) *Synthesis of* $[OsCl_2\{P(C_6H_{11})_2H\}_4]$.—Method as for (*a*) above, using $[NH_4]_2[OsCl_6]$ (89 mg, 0.203 mmol) and $P(C_6H_{11})_2H$ (0.2 cm^3, 1.01 mmol) in water–EtOH (1:3 v/v, 20 cm^3) (Found: C, 53.9; H, 8.35. Calc. for $C_{48}H_{92}Cl_2OsP_4$: C, 54.6; H, 8.80%). FAB mass spectrum: m/z 1055, 857 and 654; calc. for $[^{192}Os^{35}Cl_2\{P(C_6H_{11})_2H\}_4]^+$ 1054; loss of $P(C_6H_{11})_2H$ and Cl accounts for the other peaks. IR (KBr disc): 2960m, 2880m, 2330w, 1460m, 1360w, 1280w, 1240w, 1180w, 1135w, 1015m, 935w, 900w, 880w, 855w, 820w, 525w, 485m, 410w, 390w and 300w cm^{-1}.

(*g*) *Synthesis of* $[OsCl_2(PPhH_2)_4]$.—Method as for (*a*) above, using $[NH_4]_2[OsCl_6]$ (121 mg, 0.276 mmol) and $PPhH_2$ (0.13 cm^3, 1.14 mmol) in water–EtOH (1:10 v/v, 20 cm^3) (Found: C, 37.3, H, 3.70. Calc. for $C_{24}H_{28}Cl_2OsP_4 \cdot CH_2Cl_2$: C, 38.2; H, 3.85%). FAB mass spectrum: m/z 777, 702, 667, 590, 555, 480, 444 and 407; calc. for $[^{192}Os^{35}Cl_2(PPhH_2)_4]^+$ 702; loss of $PPhH_2$ and Cl accounts for all other peaks except for the peak at m/z 777 which is consistent with $[^{192}Os^{35}Cl(PPhH_2)_5]^+$. IR (CsI disc): 3050w, 2960w, 2330m, 1260m, 1485m, 1435w, 805m, 740m, 695s and 300w cm^{-1}.

References

1 R. Bartsch, S. Hietkamp, S. Morton, H. Peters and O. Stelzer, *Inorg. Chem.*, 1983, **22**, 3624; D. J. Brauer, F. Gol, S. Hietkamp, H. Peters, H. Sommer, O. Stelzer and W. S. Sheldrick, *Chem. Ber.*, 1986, **119**, 349; D. J. Brauer, F. Dorrenbach, T. Lebbe and O. Stelzer, *Chem. Ber.*, 1992, **125**, 1785.

2 For examples, see A. Bright, B. E. Mann, C. Masters, R. M. Slade and R. E. Srainbank, *J. Chem. Soc. A*, 1971, 1826; D. J. Brauer, P. C. Knuppel and O. Stelzer, *Chem. Ber.*, 1987, **120**, 81; C. W. Weston, G. W. Bailey, J. H. Nelson and H. B. Jonassen, *J. Inorg. Nucl. Chem.*, 1972, **34**, 1752; M. Baacke, O. Stelzer and V. Wray, *Chem. Ber.*, 1980, **113**, 1356; J. Vicente, M. T. Chicote and P. G. Jones, *Inorg. Chem.*, 1993, **32**, 4960; R. A. Palmer, H. F. Giles and D. R. Whitcomb, *J. Chem. Soc., Dalton Trans.*, 1978, 1671; R. A. Palmer and D. R. Whitcombe, *J. Magn. Reson.*, 1980, **39**, 371; P. Leoni, *Organometallics*, 1993, **12**, 2432.

3 R. G. Hayter, *J. Am. Chem. Soc.*, 1962, **84**, 3046; W. Levason, C. A. McAuliffe and B. Riley, *Inorg. Nucl. Chem. Lett.*, 1973, **9**, 1201; J. B. Brandon and K. R. Dixon, *Can. J. Chem.*, 1981, **59**, 1188; A. J. Carty, F. Hartstock and N. J. Taylor, *Inorg. Chem.*, 1982, **21**, 1349; T. Gebauer, G. Frenzen and K. Dehnicke, *Z. Naturforsch, Teil B*, 1992, **47**, 1505.

4 P. Leoni, M. Pasquali, M. Sommovigo, F. Laschi, P. Zanello, A. Albatini, F. Lianza, P. S. Pregosin and H. Rueegger, *Organometallics*, 1993, **12**, 1702.

5 R. J. Forder, I. S. Mitchell, G. Reid and R. H. Simpson, *Polyhedron*, 1994, **13**, 2139.

6 J. R. Sanders, *J. Chem. Soc. A*, 1971, 2991; *J. Chem. Soc., Dalton Trans.*, 1973, 743.

7 E. B. McAslan, A. J. Blake and T. A. Stephenson, *Acta Crystallogr., Sect. C*, 1989, **45**, 1811.

8 F. A. Cotton, B. A. Frenz and D. L. Hunter, *Inorg. Chim. Acta*, 1976, **16**, 203.

9 For examples, see F. A. Cotton, M. Matusz and R. C. Torralba, *Inorg. Chem.*, 1989, **28**, 1516; F. A. Cotton and R. C. Torralba, *Inorg. Chem.*, 1991, **30**, 2196 and refs. therein.

10 S. J. La Placa and J. A. Ibers, *Inorg. Chem.*, 1965, **4**, 778.

11 N. R. Champness, W. Levason, D. Pletcher, M. D. Spicer and M. Webster, *J. Chem. Soc., Dalton Trans.*, 1992, 2201.

12 W. Kuchen and H. Buchwald, *Chem. Ber.*, 1958, **91**, 2296.

13 V. D. Bianco and S. Doronzo, *Inorg. Synth.*, 1976, **16**, 161.
14 J. Cosier and A. M. Glayer, *J. Appl. Crystallogr.*, 1986, **19**, 105.
15 W. Clegg, *Acta Crystallogr., Sect. A*, 1981, **37**, 22.
16 SHELXS 86, program for crystal structure solution, G. M. Sheldrick, *Acta Crystallogr., Sect. A*, 1990, **46**, 467.
17 SHELX 76, program for crystal structure refinement, G. M. Sheldrick, University of Cambridge, 1976.
18 D. T. Cromer and J. B. Mann, *Acta Crystallogr., Sect. A*, 1968, **24**, 321.
19 PARST, M. Nardelli, *Comput. Chem.*, 1983, **7**, 95.
20 ORTEP II, C. K. Johnson, Report ORNL-5138, Oak Ridge National Laboratory, Oak Ridge, TN, 1976.
21 TEXSAN, Crystal Structure Analysis Package, Molecular Structure Corporation, Houston, TX, 1992.